Mixing Characteristics of a High-Rate Algae Pond

S.B. MILLER* and H.O. BUHR**

Department of Chemical Engineering, University of Cape Town, Rondebosch, 7700, South Africa

Abstract

In order to define an appropriate mathematical model for the flow and mixing characteristics of a high-rate algae pond, impulse-response tests were carried out on an experimental pond located at Ein Karem, near Jerusalem, at Reynolds number $\simeq 10^5$, and on two scale models of the same pond, at $2\,000 < Re < 20\,000$. Each pond consisted of a continuous rectangular channel with seven 180° bends, and was mechanically recirculated.

It was demonstrated that this type of pond is well characterised by either a dispersed-plug-flow model with dispersion numbers in the range 0,003 to 0,017, or by a tanks-in-series model. Dispersion intensities were correlated by a modified dispersion number for depth:width ratios in the range 0,18 to 0,76.

Introduction

An oxidation pond constitutes a well-established low-cost wastewater treatment process which combines the growth of algae with the purification of domestic sewage. The pond provides a symbiotic environment in which algae produce the oxygen required by aerobic microorganisms to convert organic matter into carbon dioxide, which, in turn, is used by the algae as substrate during photosynthesis. Oxidation ponds usually depend on diffusion and slow convection to transfer CO_2 and O_2 between the algae, generally growing near the surface, and the decaying sludge near the bottom of the pond. Interest in speeding up the process, particularly for the purpose of maximizing the production of protein-rich algae, has led to the development of the high-rate algae pond (HRAP), where transfer of CO_2 and O_2 is enhanced by mechanical agitation.

The HRAP conventionally takes the form of a continuous channel equipped with an aerator-mixer to provide the necessary circulation. A typical design, which has been used in California (Oswald, 1969) and Israel (Shelef, Schwarz and Schechter, 1973), is illustrated in Figure 1. Since mixing results in the suspension of sediments, light penetration is reduced and the optimum depth for the HRAP is about 400 mm as compared to 3 m for an oxidation pond.

The effectiveness of the HRAP as a means of wastewater treatment or of algal protein production depends not only upon the complex kinetic interrelationships between the concentrations of algae, bacteria, oxygen and the various substrates in the system, but also upon the nature of the flow and the quality of mixing in the process. A study of the mixing characteristics of the physical reaction system is therefore a necessary prerequisite to the development of a realistic dynamic model for the process. This paper presents the results of such an investigation carried out on a full-scale HRAP at Ein Karem, near Jerusalem, and two laboratory-scale models of the same pond. Dispersion coefficients under various operating conditions were determined by fitting the results of tracer studies to a dispersed-plug-flow model of the continuous channel system.

Modelling of a Reaction System

The two simplest ideal models for describing flow conditions in a reaction system are:

1. plug flow, where no mixing takes place in the longitudinal direction but perfect mixing is assumed over the cross-section of the flow channel, and

2. complete mixing, where the contents of the reactor are perfectly mixed, so that the composition of the exit stream is identical to that of the fluid within the reactor.

Real reactors do not achieve these idealised flow conditions. In order to allow for intermediate situations, the concepts of plug flow with superimposed longitudinal dispersion, or of a number of completely stirred tanks in series, are employed. If necessary, further sophistication may be attained by considering diffusion in two dimensions, or by introducing side capacitances, dead volumes, short-circuiting, etc.

The choice of an appropriate flow model may be made by determining the age history of each element of fluid as it passes through the reactor. This information, termed the residence time distribution (RTD) may be obtained by stimulus response techniques whereby a varying tracer concentration is imposed at the inlet and the corresponding response measured at the exit of the reactor. A suitable mathematical representation of the system is then developed by matching the characteristics of the experimental residence time curve with those of the mathematical model (Danckwerts, 1953; Levenspiel, 1972).

E(t), the residence time distribution function, is defined as the response of a system to a unit impulse of tracer material applied to the input. The most important parameters by which the RTD is characterised are (see Nomenclature):

1. The mean, viz., the first moment of the RTD about zero time:

$$\bar{\tau}_E = \int_0^\infty t\,E(t)\,dt \qquad (1)$$

For closed systems, where all the material injected eventually appears at the outlet, it follows by material balance that $\bar{\tau}_E$ is equal to the mean residence time, $\bar{\tau}$.

*Present address: IMI Institute for Research and Development, PO Box 313, Haifa 31000, Israel.

**Present address: Greeley and Hansen Engineers, 222 South Riverside Plaza, Chicago IL60606, USA.

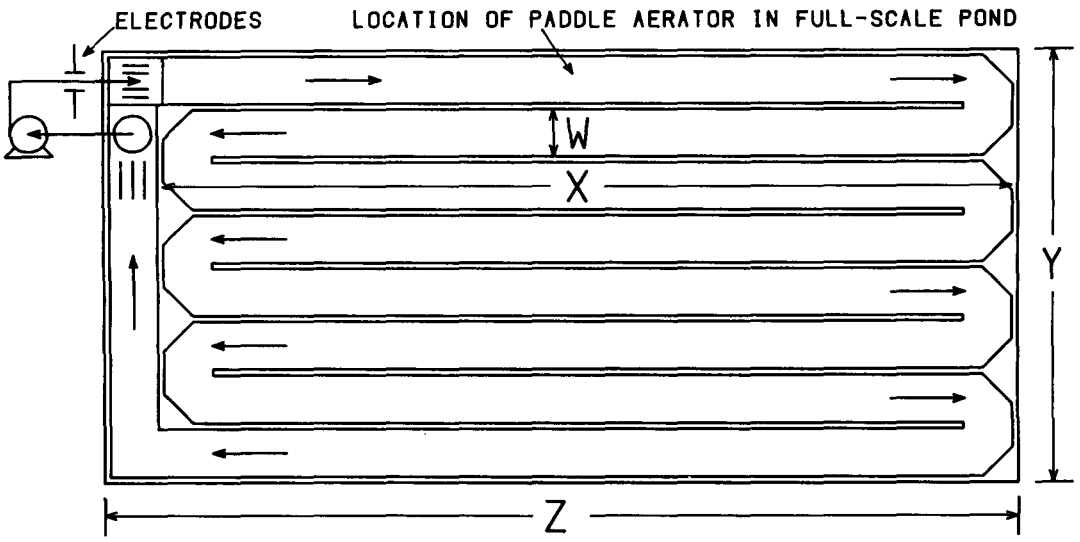

Figure 1
Scale model used in experimental studies, illustrating layout of high-rate algae pond.
For dimensions refer to Table 1.

2. The variance, viz., the second moment of the RTD about the mean:

$$\sigma^2 = {}_0\int^{\infty} (t-\bar{t}_E)^2 E(t)\,dt = {}_0\int^{\infty} t^2 E(t)\,dt - \bar{t}_E^2 \quad \ldots\ldots (2)$$

Moments of higher order may also be employed, but they often suffer from inaccuracies if the response curve has a long tail. If necessary, this problem may be alleviated by fitting an appropriate equation to the trailing portion (Gomezplata & Brown, 1968).

The quantities determined above are utilised to evaluate the parameters employed in the mathematical model. As pointed out by Clements (1969), however, a more critical assessment of the suitability of the model chosen demands that the actual time response curve be matched against the predicted impulse response of the model. In this case model parameters would be evaluated by an appropriate curve-fitting technique.

In experiments where the test input pulse to the system is not a perfect impulse function, stimulus response techniques may still be applied, provided that the shape of the input pulse is recorded. The moments of the RTD are then obtained by subtracting the values computed for the input signal from those obtained for the output (Bischoff and Levenspiel, 1962). The predicted response to a non-ideal pulse may be calculated by the use of the convolution integral:

$$C_{out}(t) = {}_0\int^{t} C_{in}(\tau)\, E(t-\tau)\, d\tau) \quad \ldots\ldots (3)$$

where C(t) is the tracer concentration and E(t), the RTD, represents the impulse response of the mathematical model.

The Dispersed Plug Flow Model

In this model, which has been extensively treated in the literature (Wen and Fan, 1975), the flow pattern is described as basic plug flow, together with a superimposed diffusion process occurring in the longitudinal direction. The latter is analogous to molecular diffusion and the rate of dispersion is proportional to the concentration gradient in the direction of flow. The effects of both turbulent mixing and radial velocity gradients are thus lumped into a single longitudinal dispersion coefficient, D.

In dimensionless form, the differential equation representing longitudinal dispersed plug flow without reaction is

$$\frac{\partial C(\Theta)}{\partial \Theta} = \frac{D}{uL}\,\frac{\partial^2 C(\Theta)}{\partial z^2} - \frac{\partial C(\Theta)}{\partial z} \quad \ldots (4)$$

The group (D/uL) is referred to as the longitudinal dispersion number, P.

The solution to this equation for an impulse input of tracer material at z = 0 depends on the boundary conditions at the points of injection and measurement. Two types of boundary condition have been extensively studied (Wehner & Wilhelm, 1956; Van der Laan, 1958; Wen and Fan, 1975), viz., the "closed vessel" condition, where no diffusion is possible in the negative direction at the inlet or in the positive direction at the outlet, and the "open vessel" condition, where the flow pattern is undisturbed at the injection and monitoring points.

The impulse response for the undisturbed or "open vessel" case can be derived analytically and is given by Levenspiel and Smith (1957) as

$$E(\Theta) = \bar{\tau}\, E(t) = \frac{1}{2\sqrt{\pi P \Theta}} \exp\left\{ - \frac{(1-\Theta)^2}{4P\Theta} \right\} \quad \ldots (5)$$

From this equation, $\bar{\tau}_E$ and σ^2 may be derived as:

$$\bar{t}_E/\bar{t} = 1 + 2P \quad \ldots\ldots (6a)$$

$$\sigma^2/\bar{t}^2 = 2P + 8P^2 \quad \ldots\ldots (6b)$$

In the case of a recirculating system, the tracer will be recorded as it flows past the measuring point at the end of the first cycle, the second cycle, etc. The output is obtained by summing the contribution from each pass (Harrell & Perona, 1968):

$$E(\Theta) = \sum_j \frac{1}{2\sqrt{\pi P\Theta}} \exp\left\{-\frac{(j-\Theta)^2}{4P\Theta}\right\} \quad \ldots (7)$$

The "closed vessel" condition, where no material is allowed to diffuse beyond the boundaries of the system, has been handled by decreasing the diffusion coefficient, D, to zero, in some acceptable fashion, at $z \leq 0$ and $z \geq L$ (Pearson, 1959; Choi and Perlmutter, 1976). This approach leads to solutions for the impulse response which are considerably more complex than equation (5) (Wen and Fan, 1975). In any but very short systems, however, or ones with relatively large dispersion numbers, the amount of material that would diffuse out through the ends of the system and hence influence the system response, is insignificant. Bearing in mind, also, that the dispersed plug flow model is only an approximation of the true flow situation in the first place, undue sophistication in the mathematical solution is not justified. For a system with a large length-to-diameter ratio, such as the HRAP, only the "open vessel" version of the dispersed plug flow model need be considered.

The Tanks-in-Series Model

An alternative representation for deviations from ideal flow is that of N equal-sized completely mixed tanks in series. The impulse response (Levenspiel, 1972) for this model is

$$E(\Theta) = \bar{t}\,E(t) = \frac{N(N\Theta)^{N-1}}{(N-1)!}\,e^{-N\Theta} \quad \ldots (8)$$

while $\bar{t}_E = t$ ... (9a)

and $\sigma^2/\bar{t}^2 = 1/N$ ... (9b)

For a recirculating system,

$$E(\Theta) = N e^{-N\Theta} \sum_j \frac{(N\Theta)^{jN-1}}{(jN-1)!} \quad \ldots (10)$$

If either of the above two models represent the system equally well, it may be seen from equations (6b) and (9b) that the relationship between the dispersion number and the number of tanks in series is

$$1/N = 2P + 8P^2 \quad \ldots (11)$$

Experimental

Tracer studies were carried out in an experimental HRAP treating domestic sewage, located at Ein Karem, near Jerusalem (Shelef, Schwarz and Schechter, 1973), as well as on two laboratory-scale models of this pond. Both scale models satisfied the criterion of geometric similarity with the Ein Karem pond and comprised a meandering channel with seven 180° bends and one 90° bend as illustrated in Figure 1. Dimensions are given in Table 1.

In the scale models, a liquid distributor was positioned at the inlet to the pond to ensure even flow. A flow-straightener located upstream of the outlet prevented vortexing and thus avoided cavitation in the centrifugal pump used for recirculation. A 10% sodium chloride solution was used as tracer and two 10 x 10 mm stainless steel electrodes were positioned in the discharge line from the pump to measure the change in conductivity of the recirculating water. Conductivity was recorded by measuring the phase change of a 1 kHz signal, rectifying, digitising to an accuracy of 1 in 1024, and printing the resulting signal at predetermined time intervals of ½ to 2 seconds. Calibration of the measuring system showed a linear relationship between printed voltages and NaCl concentration.

TABLE 1
DIMENSIONS OF ALGAL PONDS
(Refer to Figure 1)

	Small model	Large model	Full-scale pond (Ein Karem)
W, mm	65,5	130,5	1 200
X, m	1,14	2,29	20,3
Y, m	0,64	1,18	12,5
Z, m	1,25	2,47	22,5
Liquid depth, mm	20–50	24–62	380
Total length of flow path, m	9,44	18,84*	171,0

*10,00 m in case of shortened flow path

Each pond was operated as a closed recirculating system. Since flow only occurs under the influence of a liquid gradient, the model had to be inclined sideways to maintain a constant depth in the channels. Tracer tests were carried out by rapidly injecting about 4–10 ml of 10% NaCl into the pump suction at the pond outlet and recording the resulting trace for 3 to 5 cycles. In order to record the response with maximum sensitivity, the recording of the initial impulse was allowed to go off-scale. Its height was subsequently estimated by matching the area under the curve for the first pass.

The main variables investigated were the depth of liquid in the channel and the liquid flow rate, covering the Reynolds number range $2\,500 < Re < 20\,000$ and depth:width ratios between 0,18 and 0,76. In order to evaluate the influence of total length of the flow path on dispersion, a number of tests were also carried out on a "shortened" version of the larger pond, where the length of the flow path was approximately halved by positioning the exit port in the fifth channel from the inlet. The effect of channel width was examined by tests on the two scale models, one of which was half the size of the other, as well as on the full-scale pond at Ein Karem. Two tests were carried out on the latter, at $Re \simeq 10^5$ and $h/W = 0,32$, by injecting a fluorescein tracer and measuring outlet concentrations on samples collected immediately after the paddle aerator.

Results

A typical set of output data is shown in Figure 2. For clarity not all data points are included. These experimental readings were processed to obtain approximate values for mean residence

time, variance and dispersion number by numerical integration from pulse to pulse in accordance with equations (1), (2) and (6). Parameters such as these, which are obtained by integration of a global response curve, do not, however, tell us how well the chosen model represents the detailed system response. These parameters were therefore only used as starting values in an optimum search procedure, whereby the observed response was compared to the analytical impulse response, using a least-squares error criterion. The solid line in Figure 2 illustrates the quality of the fit obtained to the dispersed plug flow model as described by equation (7). Although minor deviations are noticeable, broad agreement between experimental data and the mathematical model is demonstrated.

Dispersion numbers obtained in these tests were all in the range 0,003 to 0,017. Such low values confirm the expectation that the plug flow model might be a good representation of the system and that the "open vessel" solution of the diffusion equation may be employed.

Some of the deviations exhibited in Figure 2 may undoubtedly be ascribed to the fact that the exact shape of the input disturbance could not be accurately recorded, and that a perfect impulse was accordingly assumed in the solution shown in Figure 2. The problem of non-ideality of the input pulse may be overcome, however, by noting that the output from any cycle serves as the input to the succeeding cycle, and thus the second pulse may be used to predict the shape of the third pulse, and so on, by application of the convolution integral, equation (3). Figure 3 shows the result of employing this technique, using response data as input to predict the output response of the process by convolution. The tracer concentration has been normalised with respect to the final steady-state concentration expected, viz.

$$C_f = \frac{1}{\bar{t}_o} \int^{\tau} C(t)dt \quad \ldots\ldots\ldots\ldots\ldots\ldots\ldots\ldots\ldots\ldots (12)$$

The first, imperfectly recorded, pulse is not shown. Since the second peak serves as input to the convolution, the prediction is only available from the third peak onwards. On the basis of the very good agreement obtained between prediction and experiment, it is clear that the dispersed plug flow model provides an excellent representation of the experimental system.

Similar investigations may be made to evaluate the effectiveness of the tanks-in-series model as an alternative mathematical description of the system. Computation showed that the best-fit tanks-in-series response curve agreed very closely with that of the dispersion model. As an example of the agreement obtained between model parameters, the data in Figure 2 give N = 95 as the best fit to the tanks-in-series model, in comparison with N = 91 which is obtained when the best-fit dispersion number is converted by equation (11). Because of the good agreement between the two models, it is concluded that either number-of-tanks or dispersion number may be employed to characterise flow conditions. The latter will be used in this paper.

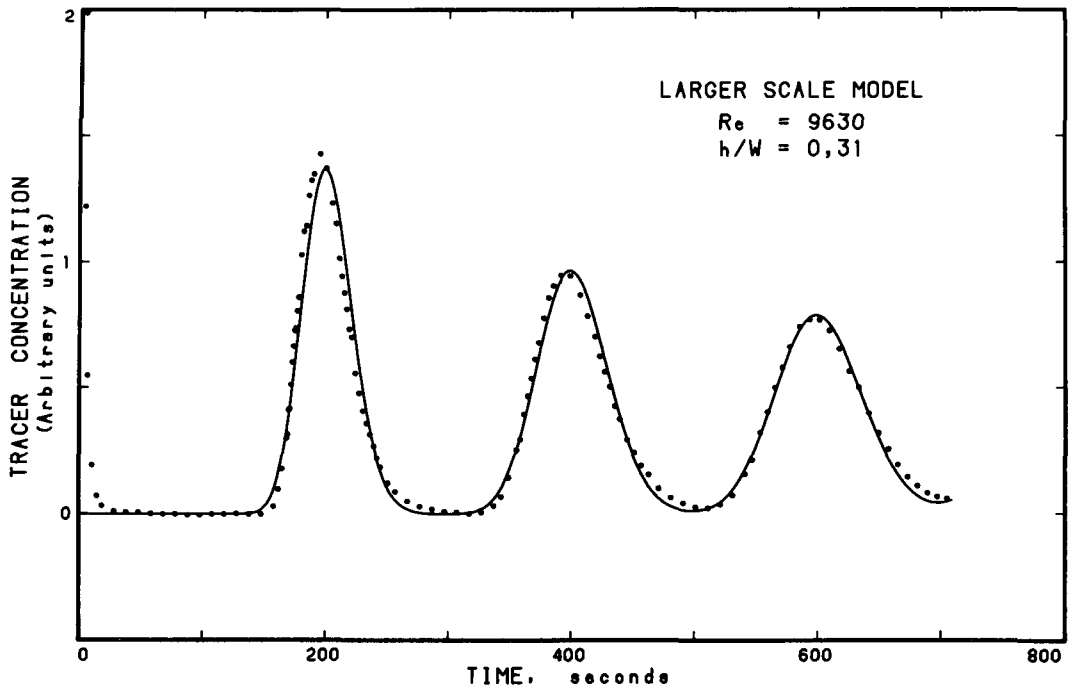

Figure 2
Reponse of HRAP to injection of tracer. ● Data (Not all data points shown); ——— Impulse response of dispersed plug flow model, eq. (7). P = 0,0051, $\bar{t}$ = 200 s.

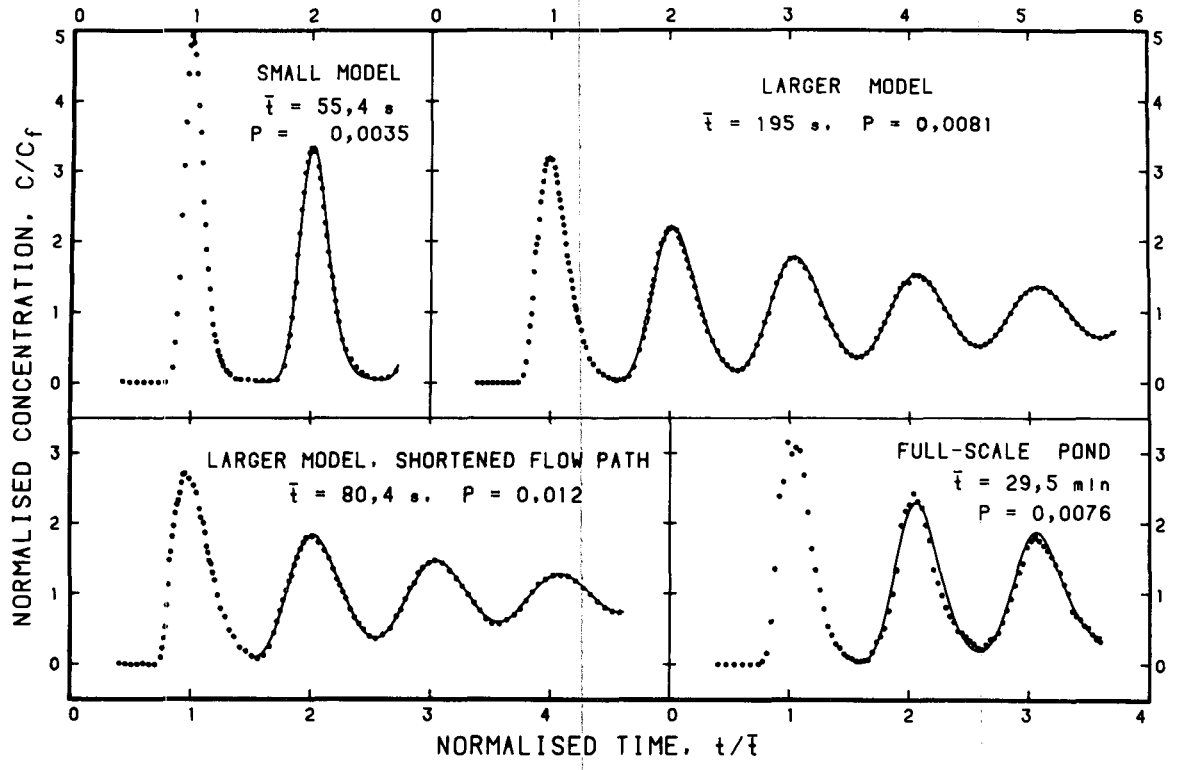

Figure 3
Quality of fit of dispersed plug flow model to experimental data, as calculated by convolution integral. (Not all data points shown.)

Dispersion Numbers

For turbulent flow in full tubes, dispersion may be represented (Levenspiel, 1958) by expressing the dispersion intensity, defined by

$$\frac{D}{ud} = \frac{D}{uL} \cdot \frac{L}{d} \quad \ldots\ldots (13)$$

as a function of Reynolds number. Wen and Fan (1975) proposed the following empirical correlation for Re > 2 000:

$$\frac{1}{D/ud} = \frac{3{,}0 \times 10^7}{Re^{2{,}1}} + \frac{1{,}35}{Re^{\frac{1}{8}}} \quad \ldots\ldots (14)$$

This relationship is presented in Figure 4, together with the experimental results for HRAP channel flow. Values of the longitudinal dispersion number, D/uL, were determined from pulse test data by the method of least-squares fitting, using the impulse response of equation (7) in conjunction with the convolution integral. The diameter, d, required in equation (13) has been taken as 4 times the hydraulic radius, i.e.

$$d = 4hW/(2h + W) \quad \ldots\ldots (15)$$

Fair agreement is shown between the experimental values for the HRAP and the equation for pipe flow, but it is evident that the data are influenced by the depth of liquid in the channel. This suggests that a further factor should be included in the correlation to account for the shape of the channel cross-section.

As an example of the use of a shape factor, the dispersion data are plotted as (D/ud)(h/W) in Figure 5, with the pipe flow equation left unchanged. An immediate improvement in the correlation is observed, although the rectangular channel data now deviate from those of pipe flow. It should be pointed out that these experiments only covered the range 0,18 < h/W < 0,76 and the indicated trend may not be valid beyond this range. The data points for the full-scale pond at Ein Karem are seen to lie somewhat above the trend suggested by the other data. These runs may have been influenced by non-ideal injection and sampling, as discussed by Levenspiel and Turner (1970). On the other hand, it is interesting to note that Cassell and Perona (1969) reported that dispersion intensity in coiled tubular reactors passed through a minimum at a Re of about 40 000. The dashed line in Figure 5 follows such a trend, but further experimental work will be needed to confirm this tendency.

Conclusions

In considering values of the dispersion intensity obtained in rectangular channels (Figure 4), it is clear that the hydraulic diameter alone does not completely account for the effect of channel shape on dispersion. Channels with relatively thin liquid layers appear to give larger amounts of dispersion, and multipli-

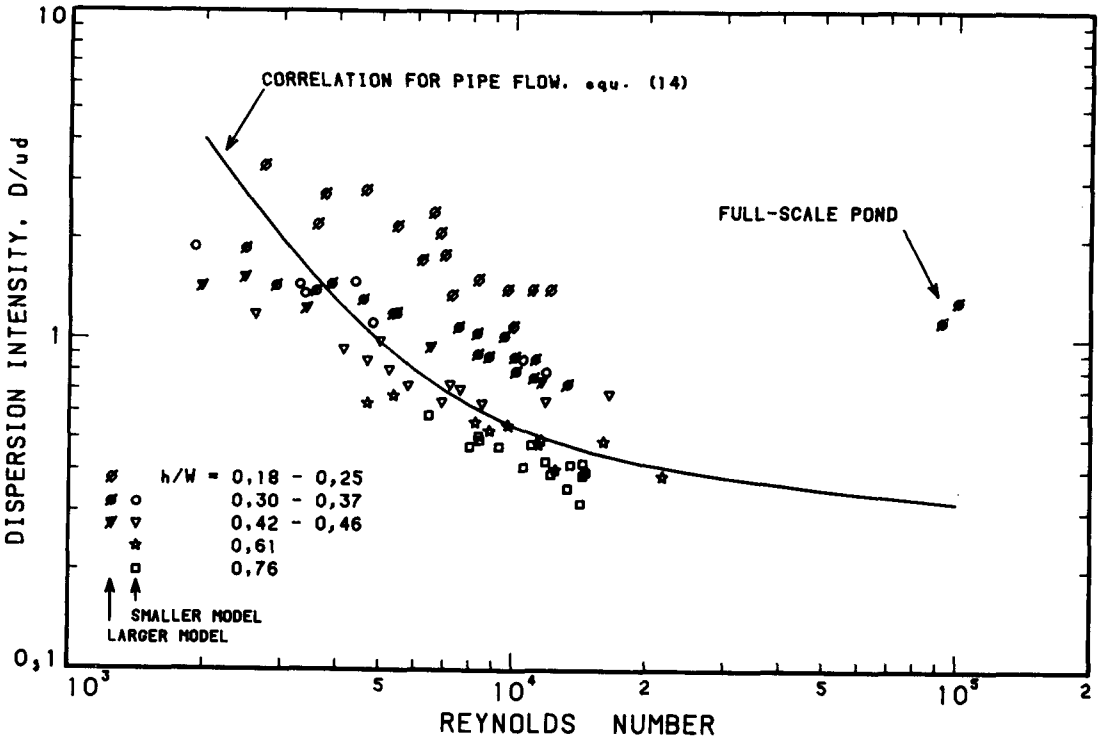

Figure 4
Experimental results for dispersion intensity in rectangular channels.

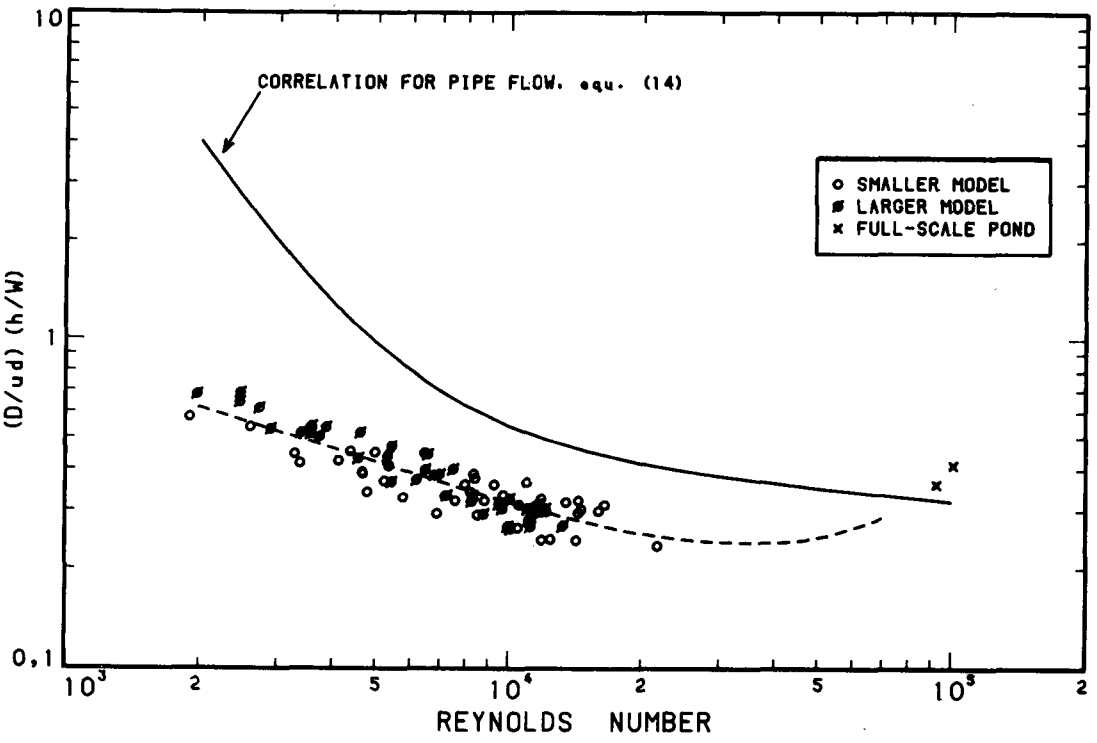

Figure 5
Correlation for dispersion intensity in rectangular channels, for 0,18 < h/W < 0,76.

cation by the factor h/W improves the correlation (Figure 5) for the tests reported here. This simple geometric ratio may not be appropriate at larger height:width ratios, where channels become very narrow, but a more general correlation must await further experimental results. The correlating factor (D/ud)(h/W) appears to be reasonable in the range $0,18 < h/W < 0,76$, and Figure 5 thus provides a means of estimating the dispersion intensity in a typical high-rate algae pond.

The linear flow velocity utilised in a HRAP will depend on the operating characteristics desired: high flow rates will give better mixing, while low flow rates would reduce suspension of sediment from the pond floor and thus allow better light utilisation throughout the pond depth. The latter condition would invalidate the assumption of complete cross-sectional mixing inherent in the dispersion model. In this study a good fit was obtained with the dispersed plug flow model for all Reynolds numbers in the turbulent region and it is considered that good vertical mixing was obtained. In contrast, results at low Re were not reproducible. Conclusions based on the dispersion model should therefore be valid as long as the flow is turbulent.

The major reason for studying dispersion in a HRAP is to obtain a mathematical description of the reaction system, together with the appropriate parameters, for use in simulation studies of bacterial and algal kinetics. It has been shown in this study that either the dispersed plug flow model or the tanks-in-series model may be employed in this instance. Figure 5 shows that the variation in the correlated dispersion intensity parameter over the range of Reynolds numbers investigated is relatively small. For a pond with the physical dimensions of the HRAP at Ein Karem, the longitudinal dispersion number will vary from 0,012 to 0,004 over the turbulent flow range. In terms of a number of equally-sized, completely mixed tanks in series, equation (11) shows that 40 to 123 tanks will be required for modelling purposes. In practice the authors found that these numbers may be substantially reduced (to about 10 – 25 tanks in series), without appreciable loss in computational accuracy.

Another point of interest is the time required to disperse (mix) a pulse input of material into the circulating fluid. "Mixing time" may be defined as the time required for the concentration anywhere within the system to reach and deviate by no more than a given fraction, γ, from the final concentration. In a study of mixing in long tanks by recirculation, Harrell and Perona (1968) determined the mixing time, based on equation (7), for various values of γ. Computed results were shown to follow a logarithmic trend of the form

$$\log(t_m/\bar{t}) = \text{constant} - \log P, \quad \ldots\ldots\ldots\ldots\ldots\ldots (16)$$

for P less than 0,04. Similarly, Khang and Levenspiel (1976) considered recirculation in a series of mixed tanks, and proposed the following equation for the amplitude of the cyclic system concentration for large N:

$$A \simeq 2 \exp \left(- \frac{2\pi^2}{N\bar{t}} t \right) \quad \ldots\ldots\ldots\ldots\ldots\ldots\ldots\ldots (17)$$

If equation (11) is substituted and the second-order term in P ignored, mixing time for small P will be given by

$$t_m/\bar{t} = \frac{-\ln(\gamma/2)}{4\pi^2 P} \quad \ldots\ldots\ldots\ldots\ldots\ldots\ldots\ldots (18)$$

Excellent agreement is obtained between equation (18) and the computed results of Harrell and Perona. By using equation (18), together with average values of the mixing intensity group from Figure 5 (dashed line), a relationship for mixing time in a high-rate algae pond may be developed, as shown in Figure 6. From this Figure, a typical mixing time in the Ein Karem pond, at Re $\simeq 10^5$, may be determined as

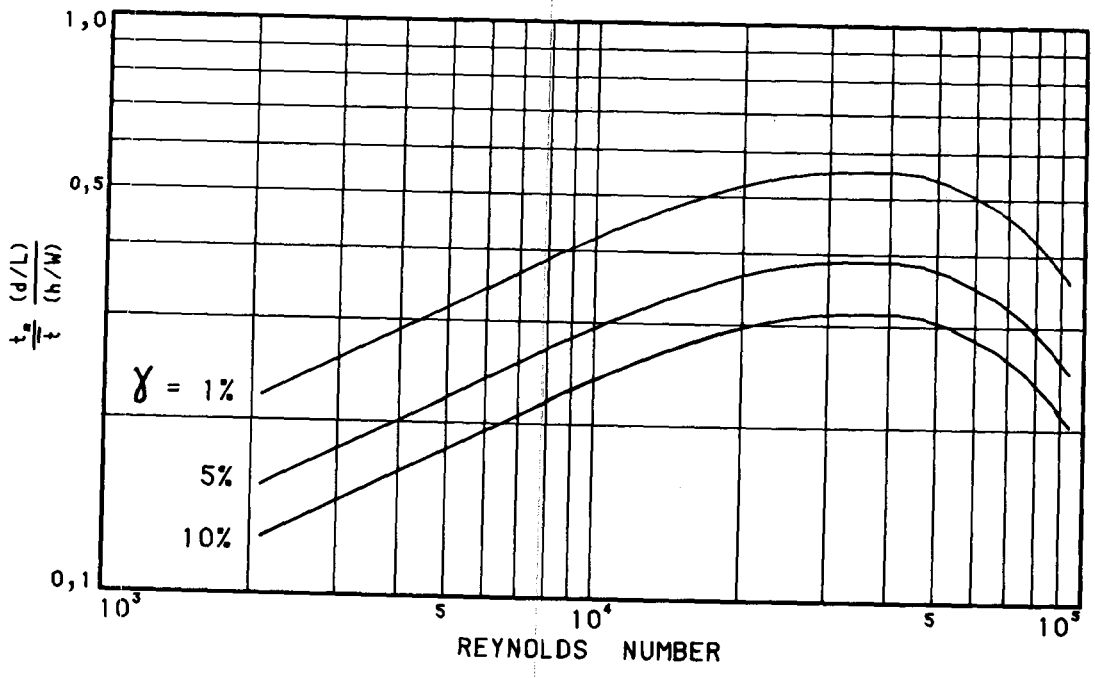

Figure 6
Time required for mixing by recirculation in a high-rate algae pond.
γ = Approach to complete mixing.

$$t_m/t = 0{,}25\frac{h/W}{d/L} = 14{,}7$$

for a 5% approach to uniformity. In this case it would take 14,7 cycles of circulation for a tracer input to be uniformly dispersed (within 5%) throughout the HRAP.

Nomenclature

- C = tracer concentration at inlet or outlet
- C_f = final steady-state concentration
- d = diameter. In case of a rectangular channel, defined as $4hW/(2h+W)$
- D = longitudinal dispersion coefficient
- E = impulse response, i.e., response of outlet concentration to an impulse disturbance at input
- h = depth of liquid in channel
- L = length of flow path between points of measurement
- N = number of equal-sized mixed tanks in series
- P = longitudinal dispersion number, D/uL
- Re = Reynolds number, du/ν
- t = time
- t_m = mixing time, i.e. time to reach and stay within a fraction, γ, of final concentration
- $\bar{t}$ = mean residence time, L/u
- $\bar{t}_E$ = time integral defined by equation (1)
- u = mean bulk velocity
- W = width of flow channel
- z = distance variable
- γ = fractional approach to final concentration
- Θ = normalised time, $t/\bar{t}$
- ν = kinematic viscosity
- σ^2 = variance, defined by equation (2)
- τ = integration variable

Acknowledgements

One of the authors (SBM) would like to express his appreciation to Professor HI Shuval and Dr G Belfort of the Hebrew University, Jerusalem, for their cooperation and assistance, and to the Bremner Fund of the University of Cape Town for financial support during his study leave.

References

BISCHOFF, K.B. and LEVENSPIEL, O. (1962) Fluid dispersion – generalization and comparison of mathematical models – I Generalization of models. *Chem. Engng Sci.* **17** 245–255.

CASSELL, R.E., Jr. and PERONA, J.J. (1969) Axial dispersion in turbulent flow through standard 90 degree elbows. *Amer. Inst. Chem. Engng J.* **15** 81–85.

CHOI, C.Y. and PERLMUTTER, D.D. (1976) A unified treatment of the inlet boundary condition for dispersive flow models. *Chem. Engng Sci.* **31** 250–252.

CLEMENTS, W.C., Jr. (1969) A note on determination of the parameters of the longitudinal dispersion model from experimental data. *Chem. Engng Sci.* **24** 957–963.

DANCKWERTS, P.V. (1953) Continuous flow systems. *Chem. Engng Sci.* **2** 1–13.

GOMEZPLATA, A. and BROWN, R.W. (1968) Axial dispersion coefficient measurement in two-phase flow. *Amer. Inst. Chem. Engng J.* **14** 657–658.

HARRELL, J.E. and PERONA, J.J. (1968) Mixing of fluids in tanks of large length-to-diameter ratio by recirculation. *Ind. Eng. Chem. Proc. Des. Dev.* **7** 464–468.

KHANG, S.J. and LEVENSPIEL, O. (1976) New scale-up and design method for stirrer agitated batch mixing vessels. *Chem. Engng Sci.* **31** 569–577.

LEVENSPIEL, O. (1958) Longitudinal mixing of fluids flowing in circular pipes. *Ind. Engng Chem.* **50** 343–346.

LEVENSPIEL, O. (1972) *Chemical reaction engineering* (2nd ed.) John Wiley and Sons Inc., New York. pp.253–296.

LEVENSPIEL, O. and SMITH, W.K. (1957) Notes on the diffusion-type model for the longitudinal mixing of fluids in flow. *Chem. Engng Sci.* **6** 227–233.

LEVENSPIEL, O. and TURNER, J.C.R. (1970) The interpretation of residence-time experiments. *Chem. Engng Sci.* **25** 1605–1609.

OSWALD, W.J. (1969) Current status of microalgae from wastes. *Chem. Engng Progr. Symp. Ser.* **65**, 93 87–92.

PEARSON, J.R.A. (1959) A note on the "Danckwerts" boundary conditions for continuous flow reactors. *Chem. Engng Sci.* **10** 281–284.

SHELEF, G., SCHWARTZ, M. and SCHECHTER, H. (1973) Prediction of photosynthetic biomass production in accelerated algal-bacterial wastewater treatment systems. In *Adv. in Water Poll. Research* (ed. Jenkins S.H.) pp.181–189, Pergamon Press, Oxford.

VAN DER LAAN, E.Th. (1958) Comments on "Notes on the diffusion-type model for the longitudinal mixing in flow". *Chem. Engng Sci.* **7** 187–191.

WEHNER, J.F. and WILHELM, R.H. (1956) Boundary conditions of flow reactor. *Chem. Engng Sci.* **6** 89–93.

WEN, C.Y. and FAN, L.T. (1975) *Models for flow systems and chemical reactors* Marcel Dekker Inc., New York.